Creation of a Thermal System for the Purpose of Locating Tumors Using Depth Thermography

Betrys Roberts

Advisor: Dr. Peter Monaghan

19 April 2024

1 Abstract

Depth thermography was a technique developed in 2020 that utilizes perpendicularly-measured temperature readings to find the depth of temperature bands within an object of interest [1]. However, the technique was developed for and has thus far been used strictly in the material sciences. This capstone is to design an experiment wherein the technique can be tested in a non-clinical setting designed to emulate a medical scenario. This is achieved by the creation of a physical system that behaves similarly to biological tissues when exposed to a localized heat source.

2 Introduction

Cancer tumors can, as a result of increased rate of angiogenesis, have a higher temperature than surrounding tissue. Other tumors have a lower temperature, due to collected necrotized tissue as the center runs out of oxygen or energy to continue to grow. These changes in temperature can be as extreme as $\pm 2^{\circ}$C away from physiological temperature [2]. This variation is large enough to be detected by infrared thermal imaging, and, therefore, the depth and position of a tumor can potentially be determined through depth thermography.

The technique uses a pair of infrared cameras positioned perpendicularly to one another. While individual cameras by themselves create only a two-dimensional (2D) representation of the object whose image was taken, this cross-layering of cameras results in one image being taken along one dimension (such as along the XZ-plane), while the second image is taken along the other (the YZ-plane). By comparing the two images, the depth of individual temperature bands or regions can be determined; where one image gives the position of these bands, the other image gives the depth, and vice versa. Together, the precise location of the hottest or coolest band of temperature, or any other band of interest, can be determined.

Infrared light does not penetrate through biological materials as readily as certain inorganic materials - only trace amounts (roughly 2-3%) of infrared light penetrates through more than 2 mm of skin or 3 cm of muscle [3]. However, if these limitations can be stressed through mathematical tricks, or if the bands can be backtracked to find an approximate location of the bands' hottest point, there is potential for the technique to be used in medical settings in at least a limited state.

This project is a continuation of E. Bilokon's "Depth Thermography of Hot Objects in Cool Environments". The objective of that project was to create a depth thermography apparatus and ensure it functioned properly by testing it with heated plastic cylinders, mugs of water, and chicken drumsticks [4]. In comparison, for this project, I will use the apparatus to test a physical system

designed to represent a human forearm. This system will have similar dimensions to a real forearm, and the materials will be selected based on their thermal properties being similar to human bone, muscle, or skin. Tumors will be represented by hand warmers injected into the system, and will be tested subcutaneously (directly under the skin layer) and intramuscularly at 2 cm and 4 cm into the muscle layer at temperatures 2°C above and below the basal temperature of the system.

3 Theory

The human body is an intricate system of tissues, organs, and bone all connected to and maintained by the cardiovascular system that pumps blood throughout. Thermoregulation, the body's ability to maintain a standard temperature of 37°C is controlled in part by vasoconstriction and vasodilation controlling blood flow [5], heat transfer from the evaporation of sweat, and convection. These processes and physical intricacies are difficult to represent with a physical, inorganic system, but the overall system can be simplified by focusing on the skin, muscle, and bone. While such a system won't have the full heat transfer capabilities of a real forearm, by focusing on a particular property of material objects known as thermal diffusivity, I can still use the system to determine the flow of temperature due to an intrusive heat source.

The higher an object's thermal diffusivity, the faster heat from an external source will spread through it. The equation for the calculation of thermal diffusivity is:

$$\alpha = \frac{K}{\rho C_p} \tag{1}$$

where α is the material's thermal diffusivity, K is the material's thermal conductivity (how well it conducts heat, ρ is the material's density, and C_p is the material's specific heat capacity (the amount of heat needed to increase the temperature of the object by 1 K or 1°C. The units of α are traditionally in $\frac{mm^2}{s}$, or $10^{-7}\frac{m^2}{s}$.

Comparing the following values for the thermal diffusivity of human skin, muscle, and bone, according to the table below:

Tissue Type	Thermal Diffusivity ($\frac{10^{-7}m^2}{s}$)
Skin	0.11
Muscle	0.16
Bone (cortical)	4.4

Table 1: Thermal Diffusivity of Human Skin, Muscle, and Bone [6] [7]

determines the values I am looking for with the materials I will gather to create the physical system.

While depth thermography can be used to find changes in temperature throughout an entire object, this project will focus on its ability to find the specific band of temperature corresponding to a hand warmer tumor injected in a known location. The temperature difference between the tissue and the tumor will be measured using the IR cameras, with the primary goal being to measure the position (subcutaneous vs 2 cm vs 4 cm intramuscular) of the tumor and the relative temperature of the tumor compared to the normal tissue. The effect these changes have on the ability of the cameras to detect the tumor within the system will also be evaluated.

4 Methods

4.1 The Depth Thermography Chamber

The chamber consists of a 42 cm x 42 cm x 42 cm box where five faces are wood and the sixth face consists of a cotton curtain to allow for access to the inside in between experiments. Set up in the center of each of two adjacent faces is an MLX90640 thermal camera connected to a Raspberry Pi2.

These cameras have a field-of-view of 55°-x35° and a resolution of 24 x 32 pixels. The Raspberry Pis utilize a Python code to take the images and determine the depth. They are connected to one another via an ethernet switch, and a computer monitor with a mouse and keyboard are connected in order to work with the code and to visualize the data [4].

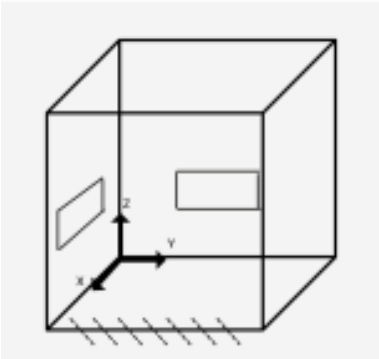

Figure 1: A Digital Mock-Up of the Chamber

Figure 2: The Chamber with System Inside

The python code shared between the two Pis causes the cameras to take images of the inside of the chamber one at a time. There is a brief delay in between one of the cameras taking an image and the other camera taking its own, in order to minimize the risk of cross-contamination of infrared waves from one camera to the next. The cameras cycle between one another until each has taken five images of the object, for a total of ten images between them. The code then analyzes the images taken, finding the brightest pixel. This pixel corresponds to the location of the object where the temperature is highest. In the +2°C tests, this will be the tumor. In the -2°C tests, this

should be somewhere within the system itself, but there will be bands of lower temperature around the tumor where it leaches heat from the former, and the same equation the python script uses to calculate the highest point will be usable manually, substituting this pocket of lower temperature.

Due to a power surge during the experiment, one of the Pis was rendered unusable. The computer itself would not turn on, and the memory chip that held all the information on it was unreadable by the other Pi. While I was able to recover the code by ddownloading a Linux extension for my personal computer and was able to procure a new Pi2, the second thermal system built proved incapable of being used for the project (this will be explained in the next section). However, for the first system that was made, the ability to rotate it between runs and take the positional and depth images separately proved a viable alternative to a more traditional depth thermographic set-up.

4.2 The Thermal System

The thermal system is comprised of a simplified forearm. There are no veins or arteries, and thus no blood flow, and no ability for it to regulate heat such as by sweating other than by passive convection of air, but the thermal diffusivity values of the selected materials are similar to those of actual skin, muscle, and bone, which should result in similar bands of temperature, even if the actual values themselves aren't identical.

The materials selected were acetal resin (or delrin), which serves as the skin, silicone rubber, used to create the muscle layer, and a pair of porcelain rods which create the forearm's skeletal structure, the ulna and radius. While the porcelain only approximates cortical bone, the narrowness of the bones within the forearm mean these bones are largely comprised of cortical bone, as opposed to trabecular bone, so my inability to find the thermal diffusivity value of the latter type of bone should not skew the results overmuch. The actual thermal diffusivity values of these materials are as follows on the table below:

Material	Thermal Diffusivity ($\frac{10^{-7}m^2}{s}$)
Delrin	0.11
Silicone rubber	0.16
Porcelain	4.41

Table 2: Thermal Diffusivity of Acetyl Resin (Delrin), Silicone Rubber, and Porcelain [8]

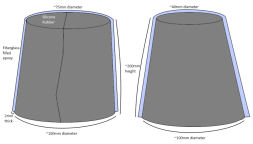

Figure 3: Outside of the system

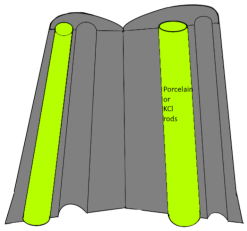

Figure 4: Cutaway of the inside

A putty mold was made sculpted around a real forearm, with proper securities put in place: the putty never touched bare skin, and only layered protection that included shrink wrap and paper. Once hardened, the mold was used to pour the silicone rubber, with the porcelain rods positioned inside it to represent the bones. A strip of delrin was cut to create the skin layer, and then bent into place around the muscle layer with the assistance of a heat gun.

Unfortunately, it was found the silicone rubber began to denature itself despite having formerly been whole, after around two weeks of use. This resulted in the replacement of the delrin skin layer with a styrofoam one, causing a loss of structure within the system itself as it shifted shape from a truncated elliptic cone to a truncated circular cone in the shape of the styrofoam cup.

A second system was later made to maintain tests with the proper skin layer. Due to the original mold being cut away from the first system post-curing, the second system was cured using a 3D-print mold.

Figure 5: System with Styrofoam Skin Layer

Figure 6: Second System, before Delrin Wrap

5 Results

The styrofoam skin system was tested first. Styrofoam has a much lower thermal diffusivity value than delrin; using the equation for thermal diffusivity, substituting $K_{styrofoam} = 0.035\frac{W}{mK}$,

$\rho_{styrofoam} = 0.037\frac{lb}{in^3} = 1024.16\frac{kg}{m^3}$, and

$C_{styrofoam} = 1131\frac{J}{kgK}$,

gives a value of

$$\alpha = \frac{K}{\rho C_p} = \frac{0.035\frac{W}{mK}}{1024.16\frac{kg}{m^3} * 1131\frac{J}{kgK}} = 0.0302\frac{10^{-7}m^2}{s} \tag{2}$$

which, while almost 4 times less than that of skin, the cup was much narrower than the delrin layer was, so I tested the system post-denaturation to see if any useable data could be obtained from it.

This has proven problematic within the experiment, and I have not been able to gather usable data yet with the exception of the subcutaneous results: going even 2 cm into the muscle results in the heat being spread too thin to penetrate the styrofoam, resulting in a blank image. As indicated below, even the subcutaneous tests result in an image not too far divorced from the blank tests (running the program without any objects inside the apparatus), as indicated below:

While there is a noticeable band of temperature within the subcutaneous model around the

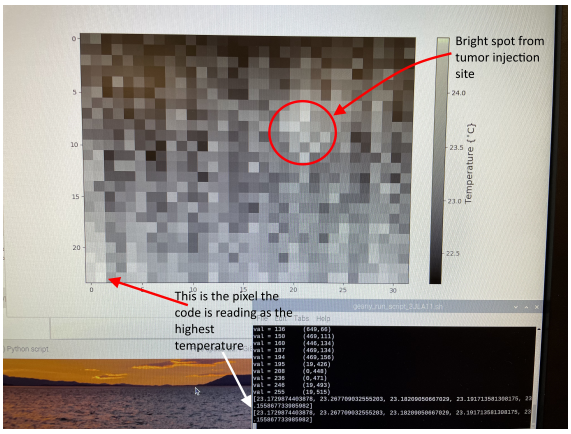

Figure 7: Styrofoam system with injected subcutaneous tumor

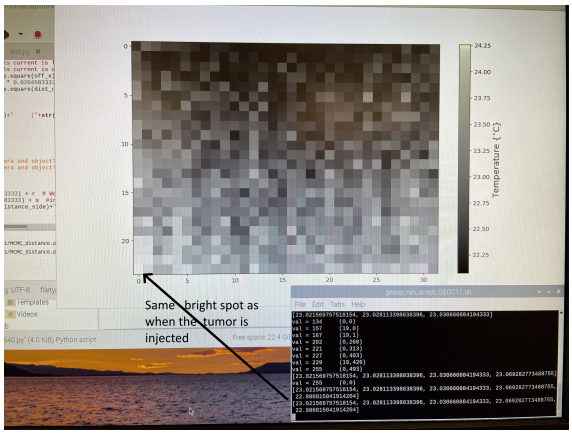

Figure 8: Background temperature of the chamber (No system or tumor inside)

location the tumor was injected, as noted in figure 8, the temperature of the model and tumor is comparable to static interference from the air. This interference could be overcome by using a full hand warmer, instead of only a small injection. The results of one of these tests is shown in Figure 9, below:

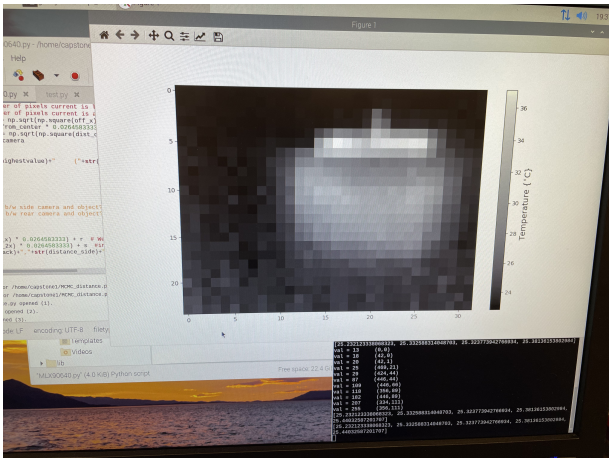

Figure 9: Full hand warmer with styrofoam skin

The region of hottest temperature is above the top of the styrofoam cup and especially above the system itself, which means the codes were analyzing the hand warmer packet itself, and not any part of the system: while bands of temperature can easily be seen within the system, they are not

physiologically useful due to the size of the tumor used.

Temperature/Distance		Subcutaneous	2 cm Intramuscular	4 cm Intramuscular
-2°	Predicted [cm]	23.42	24.83	26.25
	Calculated [cm]	—	—	—
+2°	Predicted [cm]	23.42	24.83	26.25
	Calculated [cm]	25.23	—	—

Table 3: Styrofoam System Results

The second system created was unable to be used for data collection; the silicone was too thick for the hand warmer. The needle could push into the rubber, but then the internal pressure was too great and would push the gel and needle back out before data could be taken.

6 Analysis

Unfortunately, neither system that was created was able to give good data, but as much can be learned from what doesn't work as what does. The styrofoam skin acts as too good of an insulator to be able to be used for the technique, and the silicone rubber being too thick prevented data from being taken for the second system.

The second system can be fixed by adding silicone oil to the rubber while mixing it. The two systems I created were diluted with 1:100 oil:rubber. The first system was working prior to its denaturing, while the second wasn't working properly, so if the concentration of silicone oil was increased to 1:75 or 1:50, the silicone will be softer. Another solution to the rubber being too hard is the addition of pockets of air that could be added while the system is curing; such pockets have been created in other silicone casts through the use of balloons placed in the rubber while being mixed, or specialized molds. Such a specialized mold would need to be made in two parts which

are sealed prior to the silicone being mixed and poured to cure.

In addition to the systems created not being able to use data, the low resolution of the cameras (being only 24 x 32 pixels) diminishes the ability of the code to accurately compute the true distance to the tumors due to the pixels being of fixed size and limited quantity. In solution to this, the use of a heat gun or other method to evenly warm the system prior to running tests will help reduce the effective background noise, limiting the chances of the code giving an erroneous solution. However, without obtaining better cameras with stronger resolutions, the limited pixel count will always be a limiting factor.

The system itself can also be improved on. The materials I picked were selected solely with respect to their thermal diffusivities. The three most closely matched their respective physiological counterparts, but other materials have similar enough materials they should still behave statistically similar. These other materials might, with the benefit of testing, prove better capable for creating the system than the ones I did choose. There is also another thermal property of materials I did not consider at all, which is thermal effusivity. Thermal effusivity is the opposing property to thermal diffusivity; instead of telling how quickly heat spreads through a material, thermal effusivity tells how quickly an object spreads heat to its surroundings. In addition, there are synthetic versions of the physiological materials available, such as Integra which is a synthetic skin used in medical grafts, but the use of such materials would require more time and expense than was viable for the scope of this project.

7 References

[1] Xiao, Y., Wan, C, Shahsafi, A. et al. "Depth thermography: noninvasive 3d temperature profiling using infrared thermal emission," *ACS Photonics* ***7*** (2020). https://doi.org/10.1021/acsphotonics.9b01588

[2] Shao, Q., Lundgren, M., Lynch, J. et al. "Tumor therapeutic response monitored by telemetric temperature sensing, a preclinical study on immunotherapy and chemotherapy," *Sci Rep* ***13***, 7727 (2023). https://doi.org/10.1038/s41598-023-34919-w

[3] Henderson, T., Morries, L., "Near-infrared photonic energy penetration: can infrared phototherapy effectively reach the human brain?," *Neuropsychiatr Dis Treat.* ***Aug*** (2015). doi: 10.2147/NDT.S78182

[4] Bilokon, E., Monaghan, P., "Depth thermography of hot objects in cool environments," Christopher Newport University (2023).

[5] Vuksanović, V., Sheppard, L., Stefanovska, A., "Nonlinear relationship between level of blood flow and skin temperature for different dynamics of temperature change," *Biophysical Journal* ***94*** *(2008)*

https://doi.org/10.1529/biophysj.107.127860

[6] El-Brawany, M. A., Nassiri, D. K., Terhaar, G. et al. "Measurement of thermal and ultrasonic properties of some biological tissues." *Journal of Medical Engineering & Technology* ***33*** (2009).

https://doi.org/10.1080/03091900802451265

[7] Rodríguez, G., Arenas, A., Muñoz Hernández, R., et al. "Measurements of thermal diffusivity of bone, hydroxyapatite, and metals for biomedical application," *Analytical Sciences* ***17***(2001).

[8] https://thermtest.com/thermal-resources/materials-database